INSTITUTE OF PHYSICS PUBLISHING JOURNAL OF PHYSICS: CONDENSED MATTER

J. Phys.: Condens. Matter **17** (2005) 4889–4896 doi:10.1088/0953-8984/17/32/003

Direct evidence of rigidity loss and self-organization in silicate glasses

Y Vaills[1], T Qu[2], M Micoulaut[3], F Chaimbault[1] and P Boolchand[2]

[1] Universite d'Orléans, 45067 Orleans Cedex 02 and Centre de Recherches sur les Matériaux a Haute Température, 1D avenue de la Recherche Scientifique, 45071 Orléans Cedex 02, France
[2] Department of Electrical and Computer Engineering and Computer Science, University of Cincinnati, OH 45221-0030, USA
[3] Laboratoire de Physique Théorique des Liquides, Université Pierre et Marie Curie, Boite 121, 4 Place Jussieu, 75252 Paris Cedex 05, France

E-mail: mmi@lptl.jussieu.fr

Received 8 February 2005, in final form 4 July 2005
Published 29 July 2005
Online at stacks.iop.org/JPhysCM/17/4889

Abstract

The Brillouin elastic free energy change $\Delta\Phi$ between thermally annealed and quenched $(Na_2O)_x(SiO_2)_{1-x}$ glasses is found to increase linearly for $x > 0.23$ (floppy phase), and to nearly vanish at $x < 0.18$ (stressed-rigid phase). The observed $\Delta\Phi(x)$ variation closely parallels the mean-field floppy mode fraction $f(x)$ in random networks, and fixes the two (floppy, stressed-rigid) elastic phases. In calorimetric measurements, the non-reversing enthalpy near the glass transition temperature T_g is found to be large at $x < 0.18$ and at $x > 0.23$, but to nearly vanish in the $0.18 < x < 0.23$ range, suggesting the existence of an intermediate phase between the floppy and stressed-rigid phases.

Silicate melts and glasses are important geophysical [1], optoelectronic [2] and microelectronic materials [3], and they find applications as window glass materials, optical fibres and thin-film gate dielectrics [3]. The functionality of materials often derives from their structures at different length scales. At a basic level, the molecular structure of sodium silicate $(Na_2O)_x(SiO_2)_{1-x}$ glasses consists of a network of $Si(O_{1/2})_4$ tetrahedra in which the addition of sodium oxide produces $Si(O_{1/2})_{4-m}O_mNa_m$ (or Q^{4-m} in NMR notation) local units having $m = 0, 1, 2$ and 3 non-bridging oxygen (NBO) sites attached to Na^+ ions. The addition of a few (10) mole per cent of Na_2O lowers [4] the glass transition temperature, T_g, of the base (SiO_2) material (1200 °C) sharply (to 600 °C) because of a loss in global connectivity as some Q^3 units ($m = 1$) emerge [5] at the expense of Q^4 ($m = 0$) ones. The sharp reduction of T_g destroys the mechanical equilibrium that prevailed [5, 6] in the pristine glass ($x = 0$), and drives alloyed glasses to become stressed-rigid (i.e., hyperstatic in the language of mechanical trusses). This is largely the case because the bond-bending constraint of bridging oxygen atoms that were intrinsically broken [6, 7] at 1200 °C becomes restored in the weakly alloyed glass as the T_g-values plummet to 600 °C. However, upon continued addition of Na_2O the

alloyed glass softens as network connectedness decreases, and one expects an elastic phase transition from a stressed-rigid to a floppy phase.

One can estimate the elastic phase boundary within a mean-field theory by counting the Lagrangian constraints [8, 9] per atom (n_c) due to bond-stretching and bond-bending forces. The floppy mode fraction, $f(x) = (3 - n_c)/3 = 10x/3 - 2/3$ extrapolates linearly [8, 9] to zero as n_c increases to 3 defining the phase boundary. Physically, $f(x)$ represents the count of zero-frequency (floppy-mode) solutions of the dynamical matrix in studying the normal modes of a network. In the present oxide glasses, we will show later that the condition $n_c = 3$ is met [7] when $x = 1/5$, and glass compositions at $x > 1/5$ are viewed as floppy while those at $x < 1/5$ are stressed-rigid. In the stressed-rigid phase, numerical simulations [10, 11] on random networks using a Kirkwood–Keating potential have shown that both longitudinal (C_{11}) and shear (C_{44}) elastic constants display a power-law variation as a function of $\bar{r}$ (mean coordination number equal to $8/3 - 4x/3$) or x, i.e., C_{11} or $C_{44} \simeq (\bar{r} - \bar{r}_c)^p$ with $p = 1.5(1)$ with a pronounced accuracy at higher $\bar{r}$. Such power laws have been observed in Raman mode frequency shifts examined as a function of glass composition [12, 13] but not in bulk elasticity [14–16] measurements[4]. More recently, the existence of non-mean-field effects associated with the onset of rigidity have been discovered [13]. Specifically, one has found the existence of intermediate phases [13] that open between the stressed-rigid and the floppy phase in disordered systems. The elastic phase boundary between the floppy and intermediate phase at mean network coordination number $\bar{r}_{c(1)}$ (or $x_{c(1)}$ sodium concentration), and that between the intermediate and stressed-rigid phase at $\bar{r}_{c(2)}$ (or $x_{c(2)}$), represent respectively the rigidity transition and the stress transition [13, 17].

The onset of rigidity in $(Na_2O)_x(SiO_2)_{1-x}$ glasses was examined using Brillouin scattering (BS) and temperature modulated differential scanning calorimetry (MDSC). In this paper, we show that the BS [15] reveals the mean-field behaviour of the elastic phase transition: the elastic energy change $\Delta\Phi(x)$ upon thermal annealing of the as-quenched (virgin) glasses is lowered linearly at $x > 0.24$, but is found to nearly vanish ($\simeq$0) at $x < 0.18$. The observed variation in $\Delta\Phi(x)$ closely parallels the floppy-mode fraction $f(x)$ in random networks [10], and serves to uniquely fix glasses at $x > 0.24$ to be floppy but those at $x < 0.18$ to be stressed-rigid. The stressed-rigid nature of the glasses at $x < 0.18$ is confirmed in Brillouin longitudinal ($C_{11}(x)$) and shear ($C_{44}(x)$) elastic constants that show a power-law variation with a power p respectively of 1.68(8) and 1.69(8) in fair agreement with numerical simulations [10, 11]. The non-mean-field behaviour of the underlying rigidity transition is, however, manifested in MDSC that probes glasses at all length scales. The latter technique permits one to deconvolute the endothermic heat flow near T_g, accessed from MDSC, into a reversing component that tracks the applied temperature modulation and a difference term, a non-reversing component, that does not. In these calorimetric measurements, quantified by the non-reversing enthalpy (ΔH_{nr}) at the glass transition (T_g) is found to be large at $x > x_c(2) = 0.24$ and at $x < x_c(1) = 0.18$, but to nearly vanish in the $x_c(1) < x < x_c(2)$ range. The latter range, in which $\Delta H_{nr} \simeq 0$, will henceforth be denoted as the thermally reversing window [18]. The window represents the intermediate phase. Thus, the use of two complementary probes, a mean-field (BS) one and a non-mean-field (MDSC) one, has provided a rather comprehensive view of the three elastic phases, floppy, intermediate and stressed-rigid, populated in the present prototypal oxide glass system.

Nineteen samples of $(Na_2O)_x(SiO_2)_{1-x}$ glass of 18 g weight, over the soda concentration range $0.05 < x < 0.40$, were synthesized by reacting the starting materials in a Pt–Rh

[4] In Raman studies of chalcogenides, one follows usually the frequency shift ν^2 of the A_1 stretching mode of, for example, a $GeSe_{4/2}$ tetrahedron, which is largely a measure of the network elasticity.

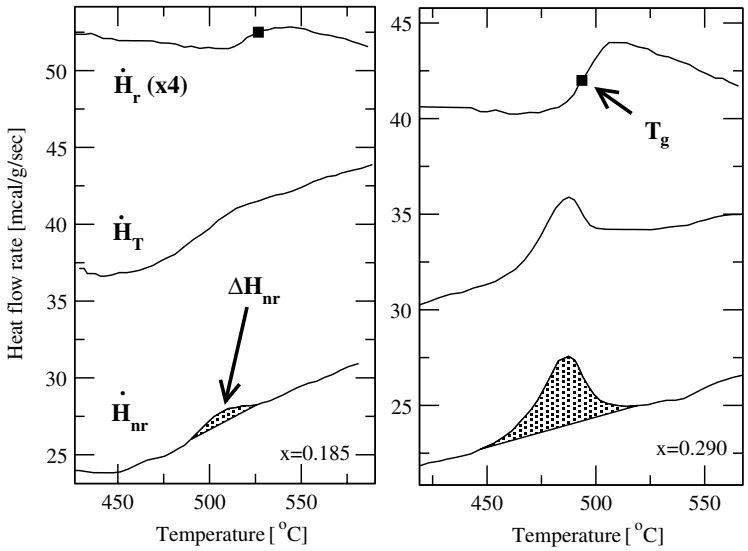

Figure 1. MDSC scan of two compositions in the $(Na_2O)_x(SiO_2)_{1-x}$ system (left panel $x = 0.185$, right panel $x = 0.290$) showing the deconvolution of $\dot{H}_T$ into $\dot{H}_{nr}$ and $\dot{H}_r$ (scale factor 4). The area under $\dot{H}_{nr}$ serves to define the non-reversing heat flow ΔH_{nr}. The T_g (filled squares) is defined from the inflexion point of $\dot{H}_r$. See the text for details.

crucible heated electrically to the 1500–1650 °C range for up to 4 h. Details of the facility are described elsewhere [19]. Melts were poured on stainless plates and checked for the absence of phase separation. FTIR examination of such quenched samples shows that they are homogeneous [20]. Glass sample cubes 8 mm across were prepared by cutting the ingots with a diamond saw and polishing the surfaces to an optical finish. Brillouin scattering was excited with $\lambda = 514.5$ nm radiation and recorded in a right-angle geometry using a pressure-scanned [19], triple-pass plane Fabry–Perot interferometer (effective finesse 70, contrast 3×10^6 and resolution power 7.6×10^5). The light source is the $\lambda = 514.5$ nm line of a single-frequency Ar-ion laser whose frequency is controlled by pressure in an iodine cell. Spectra are calibrated with a Michelson interferometer in parallel. Spectra were recorded for virgin- and annealed-glasses, and we have mostly focused on the frequency of the longitudinal and transverse acoustic modes to extract elastic constants of interest. The annealed samples were obtained by heating virgin glasses at 515 °C for 4 h [21]. Because of the hygroscopic nature of the samples, the glasses were handled in a controlled environment using glove boxes. MDSC measurements were performed [13, 18] using a model 2920 unit from TA Instruments Inc., at a scan rate of 3 °C min^{-1} and a modulation rate of 1 °C/100 s using Au pans. MDSC measurements were undertaken on vacuum annealed glasses. Figure 1 reproduces a typical scan of two sodium silicate samples in which the total heat flow $\dot{H}_T$ is deconvoluted into reversing ($\dot{H}_r$) and non-reversing $\dot{H}_{nr} = \dot{H}_T - \dot{H}_r$ components. The shaded area under the latter curve in figure 1 represents the non-reversing heat flow, ΔH_{nr}. The value of T_g was established as the inflexion point of the step seen in the reversing heat flow signal ($\dot{H}_r$).

Brillouin lineshapes observed in the glasses (figure 2) show the longitudinal acoustic (LA) mode frequency, $\nu_{LA}(x)$, to shift to a lower frequency as x increases from 0.137 to 0.20, and then to shift to a higher frequency as $x = 0.32$. Furthermore, mode frequency shifts due to annealing (broken-line curves) are small at low x (0.137) but pronounced at high x (0.32).

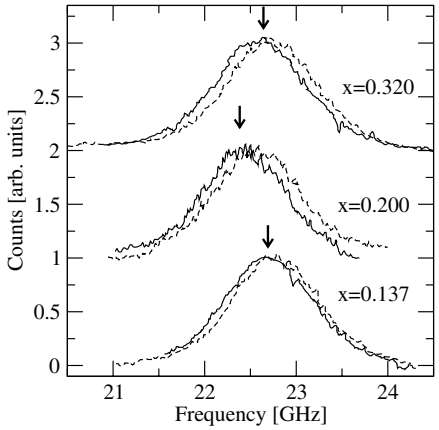

Figure 2. Brillouin lineshapes showing the longitudinal acoustic mode at indicated $(Na_2O)_x(SiO_2)_{1-x}$ glass compositions x. The mode shift between virgin (continuous line) and annealed (broken line) glasses is small at low x (0.137) and large at high x (0.32).

The longitudinal (C_{11}) and shear (C_{44}) elastic constants were obtained using the relations $C_{11} = \rho\nu_{\rm LA}^2\lambda^2/2n^2$ and $C_{44} = \rho\nu_{\rm TA}^2\lambda^2/2n^2$, where $\nu_{\rm LA}$, $\nu_{\rm TA}$, n and ρ represent the LA- and TA-mode frequencies, refractive index and mass density, respectively. The refractive index was measured using a differential path refractometer and the mass densities of virgin and annealed glasses were measured by a buoyancy method to an accuracy of ± 0.001 g cm^{-3}. Note that density changes that result from chemical alloying also influence the Brillouin lineshapes, in contrast to density changes induced by pressure or temperature [22].

Compositional trends in $C_{11}(x)$ and $C_{44}(x)$ appear in figure 3, and show C_{11} to decrease with x at first, and then to increase at $x > 0.20$, due to layered-like disilicate units [23] (adamantine) emerging as x increases to $1/3$. On the other hand, the shear elastic constant C_{44} systematically decreases as x increases to $1/3$. The lowering of the elastic free energy $\Delta\Phi$ of a network of harmonic springs upon compaction has been calculated [19]. As-quenched glasses represent networks trapped at a negative pressure, and a post-quench thermal anneal of glasses serves to compact and equilibrate them at ambient pressure. $\Delta\Phi$ can be simply expressed [19] in terms of $\Delta\rho$ and the elastic constants of the annealed glass in the hydrostatic limit as follows.

$$\Delta\Phi = \frac{1}{6}\left(\frac{\Delta\rho}{\rho}\right)^2 (3C_{11} - 4C_{44}). \tag{1}$$

As expected, changes in the elastic free energy occur in the easily deformable phase of the glasses where floppy modes proliferate. We find $\Delta\Phi$ to increase linearly at $x > 0.24$, but to vanish at $x < 0.18$, as shown in figure 3(b). The free energy of the thermally relaxed glass is lowered by an amount $\Delta\Phi$ in relation to the virgin glass. A summary of calorimetric results on the glasses appear in figure 4, with (a) displaying variations in $T_{\rm g}(x)$ deduced from the reversing enthalpy and (b) variations in the non-reversing enthalpy, $\Delta H_{\rm nr}(x)$. We find the $\Delta H_{\rm nr}$ term to be large at $x > 0.24$ and at $x < 0.18$, but to almost vanish ($\simeq$0) in the $0.18 < x < 0.23$ range.

Our interpretation of the BS results is as follows. A vibrational analysis of random networks within a mean-field theory reveals the floppy-mode fraction as a function of $\bar{r}$ to be

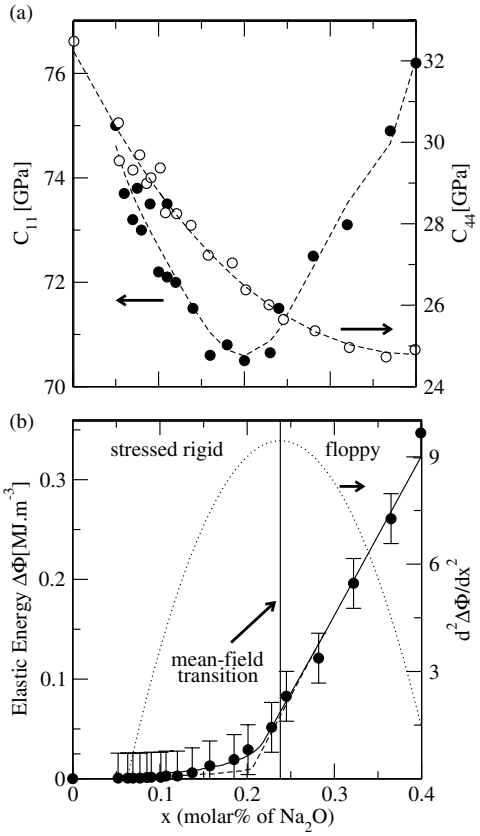

Figure 3. (a) Variations in $C_{11}(x)$ and $C_{44}(x)$ and (b) variations in elastic energy increase $\Delta\Phi(x)$ in $(Na_2O)_x(SiO_2)_{1-x}$ glasses deduced from Brillouin scattering. The continuous line and broken line give the floppy-mode fraction $f(x)$ prediction for random and self-organized networks, respectively. The second derivative of $\Delta\Phi(x)$ (dotted line, right axis) obtained from the BS results fixes the mean-field elastic phase transition at $x = 0.24$, with glasses at $x > 0.24$ being floppy.

given [10] by $f(\bar{r}) = 6 - 5\bar{r}/2$. In the present glasses, since $\bar{r} = (8 - 4x)/3$,[5] the latter equation can be written as $f(x) = \frac{10}{3}x - \frac{2}{3}$, which reveals $f(x)$ to increase linearly at $x > 1/5$ in the floppy phase, and $f(x) \simeq 0$ at $x < 1/5$ in the stressed-rigid phase, thus showing the mean-field elastic phase boundary at $x_{mf} = 1/5$. More accurate numerical simulations based on a bond-depleted amorphous Si network performed by Thorpe [10] have localized the phase boundary by plotting the second derivative of $f(\bar{r})$, which shows a maximum at $\bar{r} = 2.385$. For the case of the present oxides, the corresponding phase boundary would be at $x_{num} = 0.211$ (see footnote 5). The observed variation in $\Delta\Phi(x)$ (figure 3(b)) mimics the results of these numerical simulations of $f(x)$, and $d^2\Delta\Phi(x)/dx^2$, extracted from a polynomial fit of the data[6], shows a maximum near $x = 0.24$. Quenched glasses at $x > 0.24$ relax [19] as frozen stress is thermally annealed away by floppy or bond-rotational modes. These modes are associated with

[5] In $(Na_2O)_x(SiO_2)_{1-x}$ glasses, taking the coordination number of Si, Na and O to be respectively 4, 1 and 2, we obtain $\bar{r} = [4x + 8(1 - x)]/3 = (8 - 4x)/3$; for $\bar{r} = 2.385$, the implied threshold in $x_{num} = (8 - 3r)/4 = 0.211$ for the present oxides; for Q^4 $[Si(O_{1/2})_4]$ units, the Lagrangian constraints/atom, $n_c = (1/3)[7 + 2\frac{1}{2}4] = 3.67$; for Q^3 $[Si(O_{1/2})_3O^-Na^+]$ units, $n_c = (1/4.5)[7 + 3\frac{1}{2}2 + 2 + 1/2]/4.5 = 12.5/4.5 = 2.78$.

[6] Fourth-order polynomial fit: $\Delta\Phi = -0.000\,321\,23 + 0.1883x - 3.9435x^2 + 24.283x^3 - 25.503x^4$.

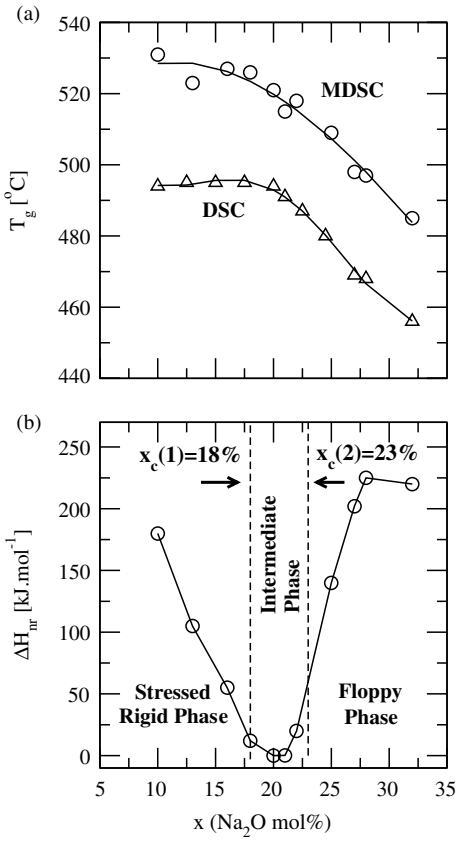

Figure 4. MDSC results on $(Na_2O)_x(SiO_2)_{1-x}$ glasses showing variations in (a) $T_g(x)$, (b) non-reversing enthalpy $\Delta H_{nr}(x)$. The DSC results were taken from [25].

the underconstrained Q^2 and Q^1 units that grow [5] precipitously at $x > 0.25$. These modes are nearly absent in the more connected glasses ($x < 0.18$). Furthermore, since our glasses were relaxed at a fixed annealing temperature of 515 °C, $\Delta\Phi(x)$ provides a measure of elastic free energy in much the same fashion that $f(x)$ is viewed [10] as the network free energy. The correlation between $\Delta\Phi(x)$ and $f(x)$ serves to uniquely fix glasses at $x > 0.24$ to be floppy and those at $x < 0.18$ to be stressed-rigid. Here we must recall that the length scale over which BS probes the elastic behaviour of glasses is set by the wavelength of the acoustic phonons that lie in the $\lambda \simeq 300$ nm range [24]. Therefore, one expects BS to probe the average elastic behaviour of the rigidity transition in the present oxide glasses as in chalcogenide glasses [15].

The calorimetric probe (MDSC) registers enthalpic changes near T_g in a glass network, and these contributions come from molecular rearrangements taking place at all length scales. For that reason, one expects to observe non-mean-field effects associated with the elastic phase transition using the thermal probe. The existence of a thermally reversing window (figure 4(b)) is an example of such an effect [18]. We find that the window sharpens and deepens upon low-temperature thermal annealing because the network stress frozen upon a quench is relieved. The window in the present oxide glasses is reminiscent of similar results in chalcogenide glasses [12, 13, 18]. The observation of a reversibility window in the present oxides leads naturally to the suggestion that glasses in the $0.18 < x < 0.24$ composition range

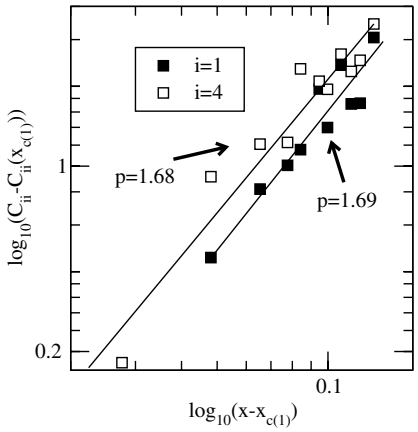

Figure 5. A log–log plot of $C_{11}(x)$–$C_{11}(0.18)$ against $(x - 0.18)$ showing a power-law variation with a power $p = 1.69(8)$ in the stressed-rigid region $(0 < x < 0.18 = x_c(1))$. Corresponding results for $C_{44}(x)$ show a power-law variation with $p = 1.68(8)$. See the text for details.

are in the intermediate phase, i.e., they are self-organized. In this range of composition, Si^{29} NMR shows [5] the concentration of underconstrained (see footnote 5) Q^3 ($n_c = 2.78$) and overconstrained Q^4 ($n_c = 3.67$) units to be comparable. Self-organization effects stem [17] from the fact that such a mix leads to an isostatically rigid global structure ($\bar{n}_c \simeq 3$).

The stressed-rigid nature of glasses at $x < 0.18$ is confirmed by the power-law variation in $C_{11}(x)$ and $C_{44}(x)$. The variation is inferred by plotting $\log(C_{11}(x) - C_{11}(x_c(1)))$ against $\log(x_c(1) - x)$, using $x_c(1) = 0.18$, and yields (figure 5) $p = p_{11} = 1.68(8)$. A similar analysis of $C_{44}(x)$ yields a power-law $p = p_{44} = 1.69(8)$. These results are in fair agreement with numerical predictions [10, 11] of $p = 1.5(1)$ in random networks as noted earlier in Raman scattering on chalcogenide glasses [12, 13]. To the best of our knowledge this is the first time one has observed a power-law variation in elastic constants for stressed-rigid glasses using a bulk probe. In BS [15] as in ultrasonic elastic moduli [14, 16], results on chalcogenide glasses show only a *linear* variation in $C_{11}(x)$. On the other hand, in Raman scattering one observes the optical elasticity (Raman mode frequency squared to tetrahedral units) with glass composition [26] to show the anticipated power-law variation. Why does one not observe the elastic power law in a bulk measurement in a chalcogenide glass, when one can observe it in the present oxide glass? Residual interactions due to dihedral angle forces and lone-pair van der Waals forces dilute the effect of first-neighbour (bond-stretching) and second-neighbour (bond-bending) forces in the chalcogenides and alter the phase transition. Long-range interactions become important at long wavelength and therefore alter the functional dependence of predictive elastic constants on $\bar{r}$. We note that the Si–O single bond strength [27] (100 kcal mol^{-1}) far exceeds the Ge–Se single bond strength (40 kcal mol^{-1}), and furthermore, lone pair interactions in oxides are likely to be much weaker than in chalcogenide glasses. Thus, it appears that a power-law variation of elastic constants is observed in those instances where first- and second-neighbour forces overwhelm residual interactions as is the case of Brillouin scattering in the oxides, or that of Raman scattering in chalcogenide [12, 13].

In summary, Brillouin scattering and MDSC have permitted the identification of the three elastic phases in $(Na_2O)_x(SiO_2)_{1-x}$ glasses; compositions at $x < 0.18$ are stressed-rigid, those in $0.18 < x < 0.23$ intermediate, and those at $x > 0.23$ floppy. A power-law variation of the longitudinal- and shear-elastic constants is observed in the stressed-rigid phase of the oxide

glasses using a bulk probe (BS) for the first time. These novel results show that the floppy to stressed-rigid phase transitions in oxide and chalcogenide glasses are remarkably similar, underscoring the commonality of the basic physics driving the formation of elastic phases in disordered systems. Our results correlate well with electrical transport measurements that show activation energy for diffusion [28] in the floppy glasses to be consistently low, and to increase steadily as the backbone becomes increasingly stressed-rigid.

Acknowledgments

This work is supported by a joint CNRS-NSF collaboration research project 13049 and NSF grant Int-01-38707 and DMR-01-01808, and DMR-04-56472.

References

[1] Stebbins J, McMillan P and Dingwell D (ed) 1995 Structure, dynamics and properties of silicate melts *Rev. Mineral* vol 32 (Washington, DC: Mineral Society of America)
[2] Suzuki S and Abe Y 1981 *J. Non-Cryst. Solids* **43** 141
[3] Lucovsky G, Yang H Y, Wu Y and Niimi H 2000 *Thin Solid Films* **374** 217
[4] Micoulaut M 1998 *Eur. Phys. J.* B **1** 277
[5] Maekawa H, Maekawa T, Kawamura K and Yokokawa T 1991 *J. Non-Cryst. Solids* **127** 53
[6] Kerner R and Phillips J C 2000 *Solid State Commun.* **117** 47
[7] Zhang M and Boolchand P 1994 *Science* **266** 1355
[8] Thorpe M F 1979 *J. Non-Cryst. Solids* **34** 153
[9] Phillips J C 1983 *J. Non-Cryst. Solids* **57** 355
[10] He H and Thorpe M F 1985 *Phys. Rev. Lett.* **54** 2107
Thorpe M F, Jacobs D J, Chubynsky M V and Phillips J C 2000 *J. Non-Cryst. Solids* **266–269** 859
[11] Franzblau D S and Tersoff J 1992 *Phys. Rev. Lett.* **68** 2172
[12] Boolchand P, Feng X and Bresser W J 2002 *J. Non-Cryst. Solids* **299** 958
[13] Selvanathan D, Bresser W J and Boolchand P 2000 *Phys. Rev.* B **61** 15061
[14] Duquesne J Y and Bellesa J 1985 *J. Physique Coll.* **46** C10 445
[15] Gump J, Finkler I, Xia H, Sooryakumar R, Bresser W J and Boolchand P 2004 *Phys. Rev. Lett.* **92** 245501
[16] Yun S S, Li H, Cappelletti R L, Enzweiler R N and Boolchand P 1989 *Phys. Rev.* B **39** 8702
[17] Micoulaut M and Phillips J C 2003 *Phys. Rev.* B **67** 104204
[18] Boolchand P, Georgiev D G and Goodman B 2001 *J. Optoelectron. Adv. Mater.* **3** 703
[19] Vaills Y, Luspin Y and Hauret G 2001 *J. Non-Cryst. Solids* **286** 224
[20] Fujita S, Kato Y and Tomozawa M 2003 *J. Non-Cryst. Solids* **328** 64
[21] For the phase diagram of sodium silicates, see Mysen B O and Richet P 2005 *Physics and Chemistry of silicates* (Berlin: Springer)
[22] Polian A, Grimsditch M and Vo-Tranh D 1997 *Phase Transit.* **63** 187
[23] Olivier Fourcade J, Phillippot E, Ribes M and Maurin M 1972 *Rev. Chem. Mineral.* **9** 757
[24] Vacher R, Pelous J and Courtens E 1997 *Phys. Rev.* B **56** R481
[25] Mazurin O V, Strelsina M V and Shvaiko-Shvaikovska T P 1987 *Ternary Silicate Glasses* (New York: Elsevier)
see also Knoche R, Dingwell D B, Seifert F A and Webb S 1994 *Chem. Geol.* **116** 1
[26] Feng X, Bresser W and Boolchand P 1997 *Phys. Rev. Lett.* **78** 4422
see also Chakravarthy S, Georgiev D G, Boolchand P and Micoulaut M 2005 *J. Phys.: Condens. Matter* **17** L1
[27] Pauling L 1960 *Nature of the Chemical Bond* (Ithaca, NY: Cornell University Press) p 85
[28] Greaves G N and Ngai K L 1995 *Phys. Rev.* B **52** 6358